Chinese Chemical Letters 33 (2022) 2507–2511

Contents lists available at ScienceDirect

Chinese Chemical Letters

journal homepage: www.elsevier.com/locate/cclet

Co-delivery of doxorubicin and curcumin *via* cRGD-peptide modified PEG-PLA self-assembly nanomicelles for lung cancer therapy

Yunchu Zhang[a,b,1], Tingting Li[a,b,1], Yuzhu Hu[a,b,1], Jing Chen[b], Yihong He[b], Xiang Gao[b,*], Yan Zhang[a,*]

[a] *Department of Thoracic Oncology, Cancer Center, State Key Laboratory of Biotherapy, West China Hospital, West China Medical School, Sichuan University and Collaborative Innovation Center for Biotherapy, Chengdu 610041, China*

[b] *Department of Neurosurgery and Institute of Neurosurgery, State Key Laboratory of Biotherapy and Cancer Center, West China Hospital, West China Medical School, Sichuan University and Collaborative Innovation Center for Biotherapy, Chengdu 610041, China*

ARTICLE INFO

Article history:
Received 22 September 2021
Revised 17 November 2021
Accepted 26 November 2021
Available online 2 December 2021

Keywords:
Doxorubicin
Curcumin
Lung cancer
Nanomicelle
Co-delivery

ABSTRACT

Lung cancer is the most common malignancy in the world, with a high mortality rate. Nevertheless, therapies to act effectively against lung cancer remain elusive. So far, chemotherapy is still the frontline treatment of lung cancer. Doxorubicin (DOX) is a broad-spectrum anti-tumor drug. However, DOX often has serious side effects and causes multi-drug resistance, which greatly limits its clinical application. In this work, biodegradable methoxy poly(ethylene glycol)-poly(lactic acid) (MPEG-PLA) and cyclo(Arg-Gly-Asp-D-Phe-Lys) (cRGD) polypeptide modified PEG-PLA (cRGD-PEG-PLA) copolymers were used for the co-delivery of curcumin (CUR) and DOX (CUR-DOX/cRGD-M). The particle size of the self-assembled drug-loaded nanomicelle approximately was 27.4 nm and the zeta potential was −2.7 mV. Interestingly, CUR can enhance the uptake of DOX by Lewis lung carcinoma (LL/2) cells. The experimental results *in vivo* and *in vitro* showed that CUR-DOX/cRGD-M combination therapy could promote apoptosis of lung cancer cells, and conspicuously inhibit the tumor growth. Our data indicate that CUR-DOX/cRGD-M will be biodegradable and sustainable, which may have potential clinical application value in the treatment of lung cancer.

Lung cancer is considered to be the second most frequently diagnosed malignancy in the world, accounting for 11.4% of all cancer diagnoses. Moreover, it is the leading cause of cancer-related mortality (18.0% of total cancer mortality) in 2020 [1–3]. The commonly used surgical resection of lung cancer has the disadvantages of operation difficulty, high risk and recurrence. Despite systemic toxicity, chemotherapy is still an indispensable treatment [4–7].

In the past few decades, researchers have found a series of chemical compounds that may be helpful in treating lung cancer. Representatively, doxorubicin (DOX) is a broad-spectrum anti-tumor drug widely used in the treatment of various cancers as a first-line chemotherapy drug [8,9]. However, DOX mediates oxidative stress in heart tissue and the dysregulation of intracellular calcium ions, which causes cell apoptosis and myocardial injury [10,11]. Therefore, the application of DOX is limited by myocardial toxicity. Curcumin (CUR) is a natural compound derived from turmeric, which is certified anti-tumor effects *in vitro* and *in vivo* [12–14]. Similarly, a significant inhibitory effect is also shown on lung adenocarcinoma cell lines with multidrug resistance (MDR) [15].

These studies have inspired us to design combination therapy strategies of DOX and CUR to synergistically inhibit the tumor growth and metastasis, maximize the therapeutic response of chemotherapy while minimizing the occurrence of MDR [16]. Besides, DOX and CUR have the same shortcomings as other traditional chemotherapeutics, such as low water solubility and low bioavailability. It is a very effective means to use amphiphilic polymer as carriers to construct drug-loaded micelles and improve drug solubility [17–19]. Methoxy poly(ethylene glycol)-poly(lactic acid) (MPEG-PLA) can self-assemble in water to form a core-shell structure. The micelle not only has an outstanding drug encapsulation efficiency and total drug release rate, but also has a preeminent biocompatibility [20–22]. After systemic administration *in vivo*, hydrophilic structures prolong the half-life of the hydrophobic drug, thereby more drugs have the opportunity to be enriched in tumor thus enhancing treatment efficacy [23–25]. cRGD peptide has been identified as an essential binding motif that can

* Corresponding authors.
E-mail addresses: xianggao@scu.edu.cn (X. Gao), zhang.yan@scu.edu.cn (Y. Zhang).
[1] These authors contributed equally to this work.

https://doi.org/10.1016/j.cclet.2021.11.076
1001-8417/

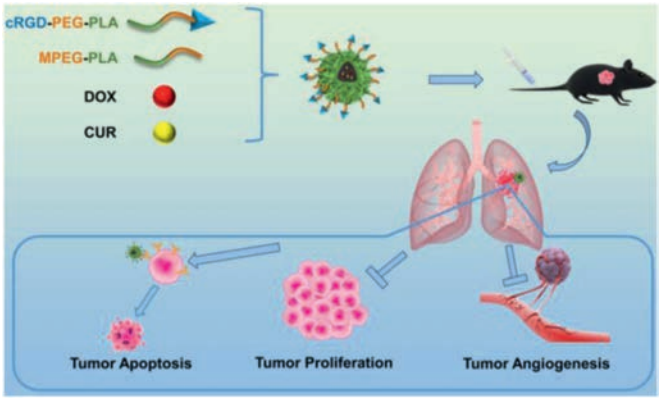

Fig. 1. Schematic diagram of research. Self-assembled nanocomposites composed of MPEG-PLA polymer, cRGD-PEG-PLA polymer, curcumin (CUR) and doxorubicin (DOX) were injected intravenously into Lewis lung carcinoma (LL/2) tumor-bearing mice, which show remarkable ability of promoting tumor apoptosis, inhibiting tumor proliferation and inhibiting tumor angiogenesis.

specifically bind integrin $\alpha_v\beta_3$ overexpressed by activated endothelial cells and tumor cells, which greatly ameliorates the targeting of nanoparticles [26–29].

Based on the above, this study combined DOX and CUR in cRGD-M nanomicelles using a self-assembled method to obtain actively tumor-targeting nanomicelles (Fig. 1). The enhanced permeability and retention effect of micelles in tumor neovascularization can enhance the cytotoxicity of tumor cells. Moreover, DOX and CUR are loaded in micelles simultaneously, which can reduce the cardiotoxicity of DOX and provide a new treatment strategy for patients with advanced lung cancer.

First of all, the molecular dynamics interactions between CUR, DOX and cRGD-PEG-PLA copolymers have been simulated by computer. As shown in Fig. S3 (Supporting information) and Fig. 2A, they gradually approached and interacted in a water environment (pH 7.0) and the environment near tumor tissue (pH 6.5). By constantly changing the position and adjusting the conformation, CUR and DOX found a suitable position for binding on cRGD-PEG-PLA. At the same time, cRGD-PEG-PLA provided appropriate binding sites for CUR and DOX by dynamically adjusting the conformation, thereby enhancing the interactions between them. In this way, through mutual coordination, a stable system has been established at 10 ns. cRGD-PEG-PLA was synthesized by a classic ring-opening polymerization [30] followed by a Michael addition reaction with cRGD (Figs. S1 and S2 in Supporting information). The drug-loaded micelles were prepared by film dispersion and ultrasonic methods. As shown in Fig. 2B, after completing self-assembly in the water phase, PLA wraps the drug molecules to form a hydrophobic core, and PEG extends outward into a hydrophilic shell. Before evaluating its cytotoxicity, the particle size and zeta potential of nanocomposites were investigated. The morphology of micelles was observed using a transmission electron microscope (TEM), which was uniformly spherical (Fig. 2D). According to the particle sizer detection, the mean hydrodynamic diameter of the nanocomposite was 27.4 nm (Fig. 2C). The polydispersity index (PDI) of the particle size was 0.133, showing a good dispersion coefficient. Moreover, the surface zeta potential of the nanocomposite was about −2.7 mV (Fig. 2E). Small nanoparticles have a stronger ability to penetrate the tumor site, while the weak negative charge on the surface of the particles can reduce the adsorption of proteins in the blood [31–33].

To investigate the cytotoxic effect of CUR/M, DOX/M and CUR-DOX/M with different concentrations, we used the MTT assay. According to the results, the cell viability of LL/2 cells was attenuated with time increase (Fig. 3A). In contrast, CUR-DOX/M had

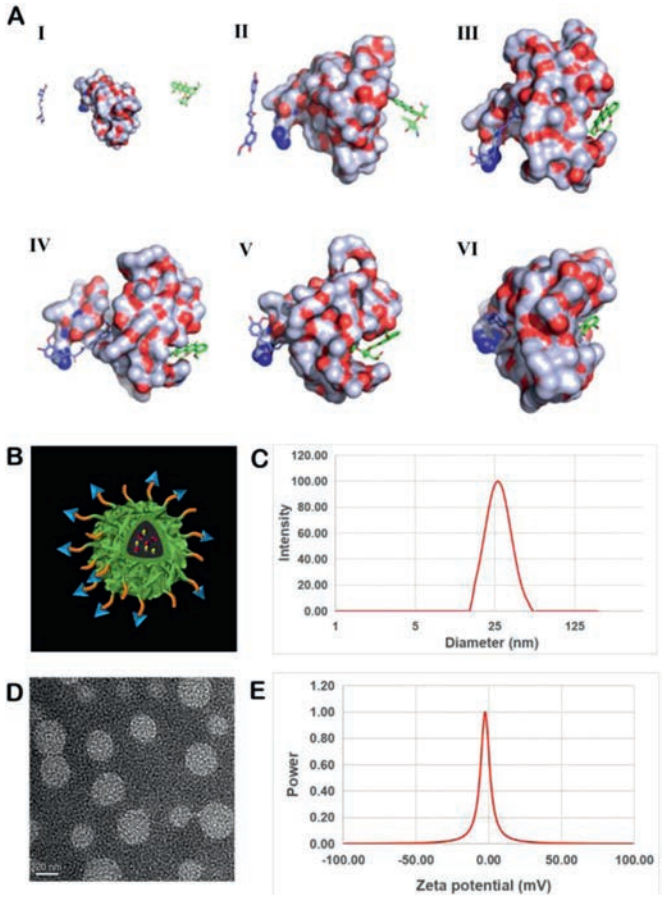

Fig. 2. Computational simulation analysis and characterization of nanocomposites. (A) Interaction modes of the cRGD-PEG-PLA copolymer, CUR and DOX in the environment near tumor tissue (pH 6.5) revealed by Langevin dynamics simulations. The nanocomposite is depicted with a solid surface. (I) The initial conformation of the cRGD-PEG-PLA copolymer complexed with CUR and DOX. The left, medial and right represent the CUR, cRGD-PEG-PLA copolymer and DOX, respectively. Conformations (II), (III), (IV), (V) and (VI) correspond to snapshots of the nanocomposite collected at 2, 4, 6, 8 and 10 nanosecond (ns), respectively. (B) Structure of the model of CUR-DOX/cRGD-M. (C) Size distribution spectrum of CUR-DOX/cRGD-M. (D) TEM image of CUR-DOX/cRGD-M. (E) Zeta potential of CUR-DOX/cRGD-M.

stronger tumor cell cytotoxicity than CUR/M and DOX/M separately, which is consistent with a previous report [34]. Owing to the autofluorescence of DOX, we performed flow cytometry on unstained LL/2 cells. LL/2 cells were treated with 0, 0.0625, 0.125, 0.25, 0.5 μg/mL of DOX/M, CUR/M or CUR-DOX/M. Intriguingly, at the same DOX concentration, we observed a significant augment in the red fluorescence intensity of LL/2 cells in CUR-DOX/M group, and cellular uptake of DOX was ameliorated with the increase in CUR/M concentration (Fig. 3C and Fig. S4B in Supporting information). Therefore, the combination of CUR and DOX showed greater toxicity, which might be due to curcumin enhancing the uptake of DOX by cells. This enhancement effect mainly comes from the inhibitory effect of CUR on P-gp-mediated drug efflux [35]. Many studies have confirmed that CUR can overcome MDR by sharply down-regulating the expression of ABC transporters associated with MDR, as well as inhibiting the ability of cancer cells to resist oxidative stress [36,37].

Meanwhile, PI/annexin-V staining flow cytometry was used to detect the apoptosis and necrosis of LL/2 cells after treatment with different concentrations of CUR/M, DOX/M and CUR-DOX/M. The results indicated that CUR/M, DOX/M and CUR-DOX/M could induce LL/2 cell apoptosis in 48 h (Fig. 3B and Fig. S4A in Supporting information). At a concentration of 0.5 μg/mL, the percentage

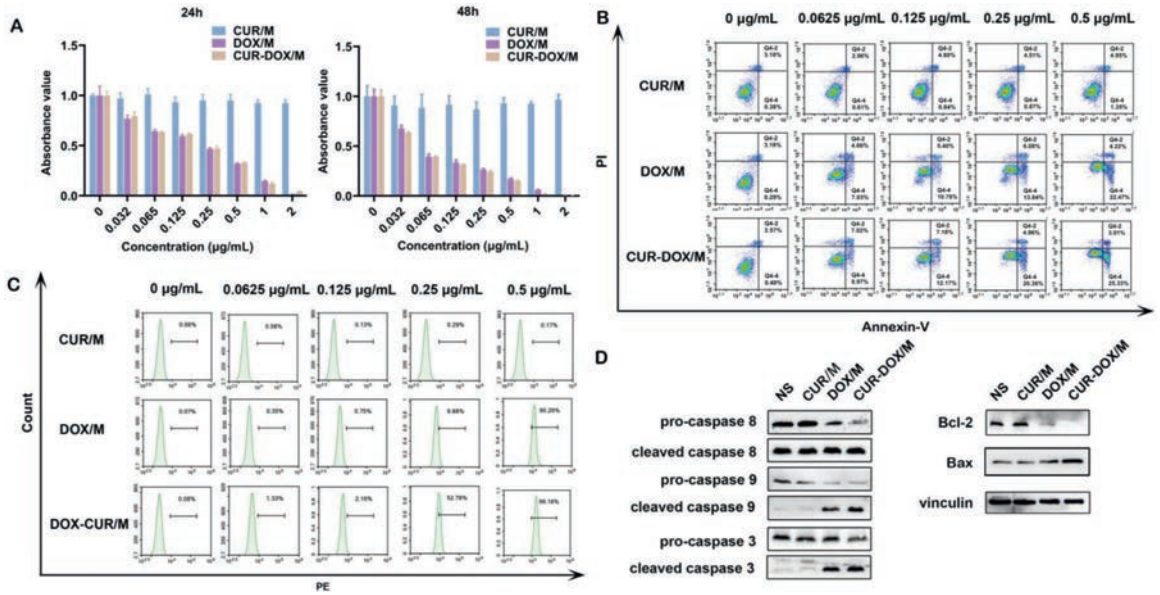

Fig. 3. *In vitro* anti-tumor effect of CUR/M, DOX/M and CUR-DOX/M. (A) Cell cytotoxicity analysis. LL/2 cells viability was detected by MTT assay after treatment with different concentrations of CUR/M, DOX/M and CUR-DOX/M at 24 and 48 h. (B) Cell apoptotic study in LL/2 cells. LL/2 cells treated with different concentrations of CUR/M, DOX/M and CUR-DOX/M for 48 h were stained by PI/annexin-V FITC to analyze cell apoptosis. (C) Effect of CUR/M on intracellular uptake of DOX/M. LL/2 cells were incubated with different concentration of nanocomposites (0, 0.0625, 0.125, 0.25 and 0.5 μg/mL) for 48 h. Then, cells were collected for uptake analysis. (D) Western blot of apoptosis-related proteins. LL/2 cells were incubated with different nanocomposites (0.5 μg/mL) for 48 h. Then, cells were collected for western blot analysis.

of annexin V^+ in LL/2 cells was 28.34% in the combination treatment group *versus* 6.30% in the CUR/M group and 26.69% in the DOX/M group, respectively (Fig. 3B). Hence, the above results confirmed that CUR-DOX/M induced more cell apoptosis and necrosis than either drug alone at the same concentration. Western blot results showed that cells treated with 0.5 μg/mL CUR-DOX/M exhibited higher expression of the apoptosis-related proteins cleaved caspase 3, caspase 8, caspase 9 and Bax, and lower expression of the anti-apoptotic protein Bcl-2 compared with the cells treated by single drug (Fig. 3D), suggesting that CUR-DOX/M promoted apoptosis of lung cancer cells.

In vivo, the anti-tumor activity of nanomicelles was firstly studied in the LL/2 subcutaneous model. The tumor-bearing mice were divided into six groups ($n = 5$): NS, Vehicle, CUR/M, DOX/M, CUR-DOX/M, CUR-DOX/cRGD-M. After being treated with the different drugs, the tumor volume of the mice was measured every 3 days. As seen in Fig. 4A, the vehicle group almost had no inhibitory effect on tumors. Compared with single-drug or non-targeted dual-drug treatment, the growth of tumors in the CUR-DOX/cRGD-M group was significantly inhibited. On the 14^{th} day post-inoculation, the targeted combination treatment group had the smallest mean tumor volume of 700 mm^3 (Figs. 4A and B) and a mean tumor weight of 0.4 g (Fig. S5A in Supporting information), yet other groups were far larger, all above 1000 mm^3 ($P < 0.001$). In addition, Fig. S5B (Supporting information) shows that there was no significant restraint of mice body weight ($P > 0.05$). Therefore, we concluded that targeted combination therapy could prevent primary tumor progression more effectively than the monotherapy.

The CUR-DOX/cRGD-M not only had a significant effect on LL/2 subcutaneous tumors, but also had a more significant effect on LL/2 pulmonary metastases. The pulmonary metastases model was established by injecting LL/2 cells into the tail vein and the mice were treated since the 7^{th} day. On the 22^{nd} day, the mice were sacrificed and their lungs were removed for metastatic nodules counting and subsequent tissue sections preparation. According to the photographs (Figs. 4C and D), no visible pulmonary nodules were found in lungs from mice treated with CUR-DOX/cRGD-M, while multiple metastatic nodules could be seen in the lungs from other groups (Figs. S6A and B in Supporting information). Furthermore, the pathological sections of the lung shown by H&E staining also had a significant difference (Fig. 4E). These results indicated that treatment with CUR-DOX/cRGD-M could remarkably inhibit the pulmonary metastases. In addition, Fig. S6C (Supporting information) shows that there was no significant restrain of mice body weight ($P > 0.05$). All animal experiments were approved by the Animal Experimental Ethics Committee of State Key Laboratory Biotherapy (SKLB), Sichuan University (No. SKLB 2020–1016).

Regardless of whether it was in the subcutaneous tumor model or the pulmonary metastases model, the CUR-DOX/cRGD-M group showed a better effect than the CUR-DOX/M group, mainly due to the accumulation of cRGD-PEG-PLA micelles in the tumor via receptor active targeting and nanoparticle enhanced permeability and retention (EPR) effect. According to previous reports, integrin $\alpha_v\beta_3$ is markedly up-regulated in various types of tumor cells and activated endothelial cells to promote tumor angiogenesis, whereas it is not up-regulated at all or rarely in resting vascular cells and other normal cells [38,39] . For lung cancer, integrin $\alpha_v\beta_3$ is widely overexpressed on tumor neovasculature and tumor cells. Therefore, cRGD-micelles that can specifically bind to receptors exhibit superior treatment effects.

We detected the proliferation of tumors in tumor tissue sections of different treatment groups using Ki67 staining. Generally, a higher Ki67 index indicates that the tumor is more active in proliferation and poorer prognosis. After treatment with CUR/M, DOX/M, CUR-DOX/M or CUR-DOX/cRGD-M, the Ki67 index was observably diminished, indicating that all four treatments had proliferation inhibition effects. Notably, the DOX-CUR/M group had the lowest Ki67 index among treatment groups (Fig. 5A and Fig. S7B in Supporting information). Additionally, angiogenesis was analyzed by CD31 immunohistochemical staining. As shown in Fig. 5B and Fig. S7A (Supporting information), the CUR-DOX/cRGD-M group had the lowest number of vessels ($P < 0.001$). At the same time, TUNEL apoptosis staining was used to evaluate the apoptosis of tumor cells in the LL/2 subcutaneous model. As shown in Fig. 5C and Fig. S7C (Supporting information), the CUR-DOX/cRGD-M group had the highest apoptotic percentage than other groups ($P <$

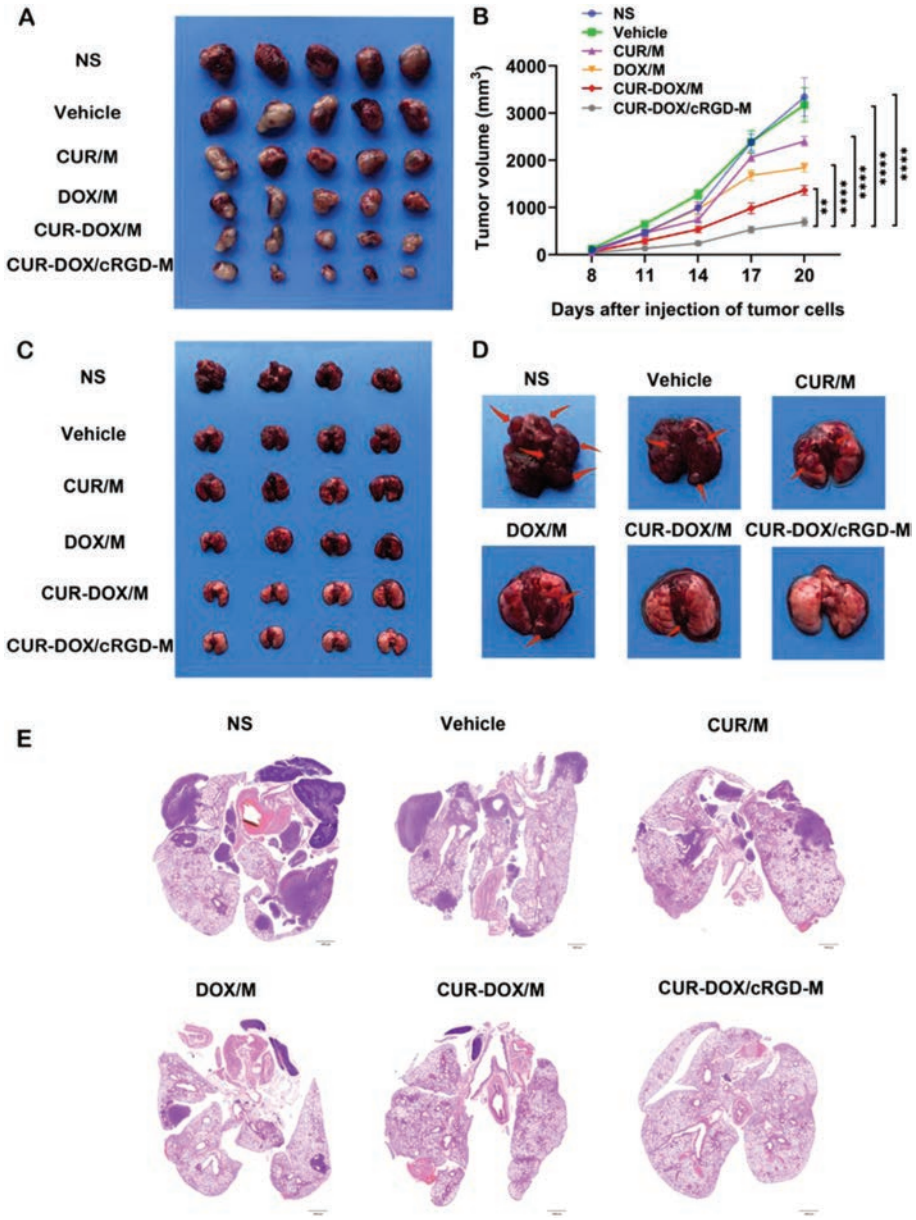

Fig. 4. Anti-tumor effects in the LL/2 subcutaneous model and pulmonary metastasis tumor model. (A) Images of the LL/2 subcutaneous tumors from different groups. (B) Tumor growth curve during the treatment. $n = 5$, $^{**}P < 0.01$, $^{****}P < 0.0001$. (C) Images of the LL/2 pulmonary metastasis tumor model from different groups. (D) Lung metastatic nodules on LL/2 pulmonary metastasis tumor model from different groups. (E) Representative histopathological sections of the lung from each group. Scale bar: 1000 μm.

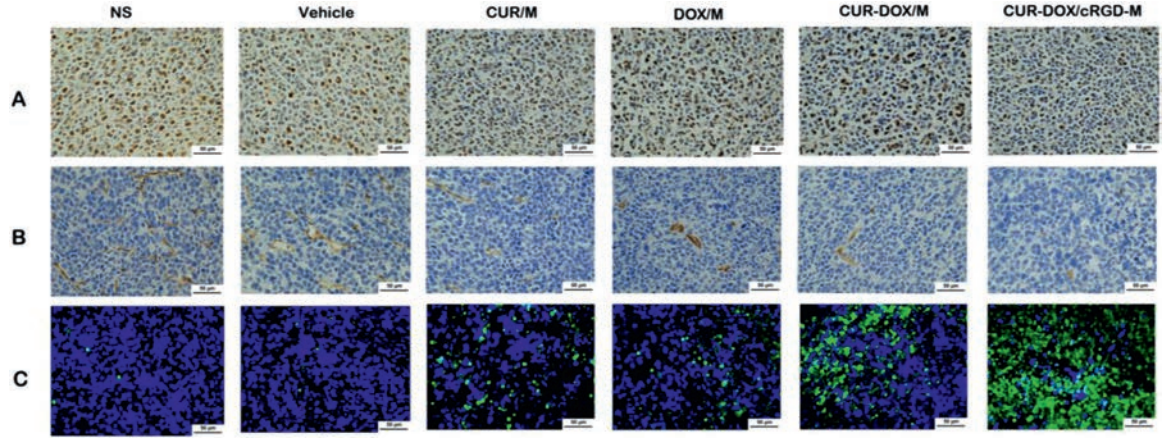

Fig. 5. Tumor proliferation, angiogenesis and apoptosis assays *in vivo*. (A) Ki67 staining was performed in tumor tissue sections of different groups to visualize tumor proliferation. (B) CD31 staining was applied to analyze tumor angiogenesis. (C) TUNEL staining was conducted to evaluate tumor apoptosis. Scale bar: 50 μm.

0.001). The results of immunohistochemical staining demonstrated that CUR-DOX/cRGD-M therapy can effectively inhibit cell proliferation and angiogenesis *in vivo*, and promote apoptosis.

In the anti-tumor experiment, because micelles can efficiently deliver drugs to the lesion, we used a lower dose (3 mg/kg) than the usual treatment (5 mg/kg), which improved the safety without affecting the treatment efficacy. To evaluate the safety of CUR-DOX/cRGD-M in the treatment of lung cancer, we performed H&E staining of vital organs and blood biochemical analysis. After treatment, the vital organs of the treated mice showed no abnormal histopathological changes on H&E staining, such as necrosis, injury or inflammation, suggesting CUR-DOX/cRGD-M was well tolerated by mice (Fig. S8 in Supporting information). In addition, blood biochemical analyses showed no obvious differences (Fig. S9 in Supporting information). The initial safety evaluation confirmed that the combination of CUR and DOX delivered by cRGD-M micelles were well tolerated in mice without noticeable side effects and systemic toxicity.

In summary, we developed a new strategy to construct CUR-DOX/cRGD-M as an efficient combination therapy nanodrug for lung cancer treatment. It exhibited good tumor-targeting capability, well biodegradability and biocompatibility. Combined treatment displayed enhanced anti-tumor and anti-metastatic ability in lung cancer therapy. Our results suggest CUR-DOX/cRGD-M has great potential for the treatment of lung cancer and provide a basis for clinical drug development.

Declaration of competing interest

The authors declare no conflict of interest.

Acknowledgments

This work was supported by the National Natural Science Foundation of China (No. 82172630), the Key R&D Projects of the Science and Technology Department of Sichuan Province (Nos. 2021YFS0237, 2020YFS0213) and the 1·3·5 Project for Disciplines of Excellence, West China Hospital, Sichuan University (No. ZYJC21022).

Supplementary materials

Supplementary material associated with this article can be found, in the online version, at doi:10.1016/j.cclet.2021.11.076.

References

[1] H. Sung, J. Ferlay, R.L. Siegel, et al., CA Cancer J. Clin. 71 (2021) 209–249.
[2] A.A. Thai, B.J. Solomon, L.V. Sequist, et al., The Lancet 398 (2021) 535–554.
[3] R.D. Neal, F. Sun, J.D. Emery, et al., BMJ 365 (2019) l1725.
[4] F.R. Hirsch, G.V. Scagliotti, J.L. Mulshine, et al., The Lancet 389 (2016) 299.
[5] Y.W. Kong, E.C. Dreaden, S. Morandell, et al., Nat. Commun. 11 (2020) 4124.
[6] S. Wang, G. Yu, Z. Wang, et al., Adv. Mater. 30 (2018) 1803926.
[7] X. Jing, F. Yang, C. Shao, et al., Mol. Cancer 18 (2019) 157.
[8] F. Roncato, F. Rruga, E. Porcu, et al., Nat. Commun. 9 (2018) 4070.
[9] L. Zhu, W. Ma, M. Zhang, et al., Nat. Commun. 9 (2018) 1283.
[10] K.T. Sawicki, V. Sala, L. Prever, et al., Annu. Rev. Pharmacol. Toxicol. 61 (2021) 309–332.
[11] J.A. Pan, H. Zhang, H. Lin, et al., Redox. Biol. 46 (2021) 102120.
[12] J. Zhang, S. Li, F.F. An, et al., Nanoscale 7 (2015) 13503–13510.
[13] Y. Xi, J. Ge, M. Wang, et al., ACS Nano 14 (2020) 2904–2916.
[14] J. Lal, S.K. Gupta, D. Thavaselvam, et al., Chin. Chem. Lett. 27 (2016) 1067–1072.
[15] F. Yu, Y. Tu, S. Luo, et al., Nano Lett. 21 (2021) 2216–2223.
[16] P. Zhang, J. Li, M. Ghazwani, et al., Biomaterials 67 (2015) 104–114.
[17] X. Zheng, J. Xie, X. Zhang, et al., Chin. Chem. Lett. 32 (2021) 243–257.
[18] M.E. Davis, Z. Chen, D.M. Shin, et al., Nat. Rev. Drug Discov. 7 (2008) 771–782.
[19] J. Xie, Y. Lu, B. Yu, et al., Chin. Chem. Lett. 31 (2020) 1173–1177.
[20] Z. Li, D. Yuan, G. Jin, et al., ACS Appl. Mater. Interfaces 8 (2016) 1842–1853.
[21] S.W. Lee, M.H. Yun, S.W. Jeong, et al., J. Control. Release 155 (2011) 262–271.
[22] T. Yu, W. Nie, Z. Hong, et al., Adv. Funct. Mater. 31 (2021) 2100715.
[23] J. Guo, L. Gao, H. Su, et al., Biomaterials 32 (2011) 8010–8020.
[24] M.T. Manzari, Y. Shamay, H. Kiguchi, et al., Nat. Rev. Mater. 6 (2021) 351–370.
[25] J. Huang, X. You, P. Xin, et al., Chin. Chem. Lett. 32 (2021) 1737–1742.
[26] Y. Zou, J. Wei, Y. Xia, et al., Signal Transduct. Target. Ther. 3 (2018) 32.
[27] Y. Luo, X. Zheng, P. Yuan, et al., Bioact. Mater. 6 (2021) 4065–4072.
[28] K. Wang, Y. Xiang, W. Pan, et al., Chin. Chem. Lett. 33 (2022) 793–797.
[29] T. Sun, Y. Ding, X. Wang, et al., Nano Lett. 20 (2020) 5275–5283.
[30] S. Kaihara, S. Matsumura, A.G. Mikos, et al., Nat. Protoc. 2 (2007) 2767–2771.
[31] H. Cabral, Y. Matsumoto, K. Mizuno, et al., Nat. Nanotech. 6 (2011) 815–823.
[32] S.D. Perrault, C. Walkey, T. Jennings, et al., Nano Lett. 9 (2009) 1909–1915.
[33] Y. Matsumoto, J.W. Nichols, K. Toh, et al., Nat. Nanotech. 11 (2016) 533–538.
[34] F. Abedi, S. Davaran, M. Hekmati, et al., J. Nanobiotechnology 19 (2021) 18.
[35] S. Dallavalle, V. Dobricic, L. Lazzarato, et al., Drug Resist. Updat. 50 (2020) 100682.
[36] P. Chen, H.P. Huang, Y. Wang, et al., J. Exp. Clin. Cancer Res. 38 (2019) 254.
[37] X. Dong, Y. Sun, Y. Li, et al., Small 17 (2021) 2007672.
[38] S. Gao, Y. Wei, N. Liu, et al., J. Clin. Oncol. 34 (2016) e20048.
[39] X. Jin, N. Liang, M. Wang, et al., Radiology 281 (2016) 958–966.